

# Real-Time Kinematic Performance Evaluation of Mosaic-H GNSS Receiver on UAV Platforms Under Diverse Environmental Conditions

Mnar Hmdy Abdalazeez Salem Saad, Ahmed Wasiu Akande, Odai Redhwan Mohammed Othman and Dongkai Yang

Beihang and RCSSTEAP, Hangzhou, China

Emails: mnar102310@gmail.com, ahmedwasiu24@buaa.edu.cn, odai7@buaa.edu.cn and edkyang@buaa.edu.cn

Abstract: This paper presents a comprehensive evaluation of the Mosaic-H GNSS receiver's Real-Time Kinematic (RTK) performance when integrated with unmanned aerial vehicle (UAV) platforms. Through systematic testing across varied operational environments including open-sky, urban canyon, and forested areas, we characterize the receiver's positioning accuracy, fix reliability, and multipath resilience. Our experimental methodology employed a precisely configured base station broadcasting RTCM corrections via Port 8105, with the UAV-mounted receiver maintaining centimeter-level accuracy in optimal conditions. Results demonstrate an 88.2% RTK fixed solution rate across all test scenarios, with horizontal accuracy averaging 3.1 cm in open environments. Notable findings include identification of critical operational thresholds: maintaining >10m clearance from buildings prevents multipath-induced degradation, canopy coverage exceeding 70% triggers fallback to float solutions, and vehicle speeds above 8 m/s challenge phase tracking capabilities at 5 Hz update rates. The multipath impact score correlation analysis revealed strong relationships between environmental factors and positioning quality (R<sup>2</sup>=0.87), enabling predictive mitigation strategies. These findings establish operational guidelines for reliable centimeter-accuracy UAV navigation in complex environments, with direct applications to

precision agriculture, infrastructure inspection, and autonomous aerial surveying.

**Keywords:** (RTK GNSS, UAV navigation, Mosaic-H receiver, multipath mitigation, positioning accuracy)

### I. INTRODUCTION

Unmanned Aerial Vehicles (UAVs) have become indispensable tools in numerous domains, including precision agriculture, environmental monitoring, infrastructure inspection, and autonomous surveying. Among the available positioning technologies, Real-Time Kinematic (RTK) Global Navigation Satellite System (GNSS) stands out as the gold standard for achieving centimeter-level positioning accuracy in aerial applications. By integrating RTK-GNSS with UAV platforms, operators can achieve precise, realtime trajectory estimation essential for photogrammetry, LiDAR mapping, 3D reconstruction, and autonomous navigation.

RTK GNSS enhances standard GNSS by using carrierphase measurements and differential corrections from a reference base station to resolve integer ambiguities, enabling precise real-time trajectory estimation. This capability is essential for tasks such as photogrammetry, LiDAR mapping, 3D reconstruction, and autonomous navigation

However, UAV operations introduce additional complexities that can affect RTK performance. High-

frequency vibrations from motors and propellers induce phase noise in GNSS carrier signals, degrading RTK fix stability. Rapid UAV maneuvers, such as hovering, banking, and acceleration, frequently cause signal cycle slips and temporary fix loss. In dense urban environments, reflected signals introduce constructive and destructive interference, inflating positioning errors, whereas forested areas exacerbate signal attenuation, reducing satellite visibility and increasing fix ambiguity resolution times [1]. Onboard electronics, such as cameras, flight controllers, and power distribution boards, also generate electromagnetic interference (EMI) that can affect GNSS front-end sensitivity and degrade carrier-phase tracking. Additionally, RTK performance relies heavily on continuous, low-latency corrections from a base station or network, and even minor delays in correction streams can cause float solutions or total fix loss during UAV operations [2], [27].

Modern multi-frequency receivers, such as the Mosaic-H, are equipped with advanced algorithms designed to mitigate these issues, but their performance under the combined stress of UAV dynamics and harsh environmental conditions remains insufficiently characterized. This limitation underscores the need for a comprehensive evaluation of UAV-integrated RTK systems in real-world scenarios.

Recent studies have attempted to address these challenges, producing valuable insights into UAV RTK performance under specific conditions. Integrating RTK-GNSS with multispectral photogrammetry has achieved sub-millimeter horizontal and vertical accuracy (~4 mm 3D) in drone-based topographic mapping, demonstrating the upper limits of RTK performance in unobstructed environments [1]. Punzet and Eibert [3] investigated the influence of antenna ground plane size and material on UAV-mounted RTK systems and found that suboptimal ground plane designs can increase positional error by up to 35%, highlighting the importance of hardware optimization. A 2025 study evaluated RTK-GNSS performance under dense tree canopy and reported horizontal accuracy variations between 1 cm and 12 cm, depending on canopy density and UAV altitude [4]. Similarly, Suzuki et al. [5] proposed a multi-antenna GNSS approach for UAVs operating in multipath-rich urban environments, achieving ≈5 cm accuracy despite frequent satellite signal blockages. Moreover, while comprehensive reviews confirm that modern multifrequency receivers can achieve geodetic-grade performance in open-sky conditions [6], specific evaluations reveal important distinctions. Performance benchmarks for popular receivers like the u-blox ZEDshow centimeter-level accuracy in open environments but significant degradation to decimeterlevel errors in urban and forested settings [7]. Similarly, studies of geodetic-grade systems highlight their superior resilience in challenging conditions, though often at substantially higher cost [8]. There is still no comprehensive, cross-environment evaluation of UAV-integrated RTK performance using modern multi-frequency receivers like the Mosaic-H across open-sky, urban canyon, and forested contexts.[9].

To address this gap, this study presents a comprehensive experimental assessment of the Septentrio Mosaic-H multi-frequency GNSS receiver integrated into a UAV platform. Unlike previous work, we evaluate RTK performance across three distinct environments—open-sky, urban canyon, and forest canopy—capturing a full spectrum of operational challenges. The study introduces a novel multipath scoring methodology based on carrier-phase residuals, signal-to-noise ratios (SNR), and geometric dilution of precision (GDOP), enabling real-time assessment. Furthermore, quantitative thresholds for UAV RTK performance are established to support predictive mission planning and improve navigation reliability. The operational thresholds and guidelines derived from this study are directly applicable to precision agriculture, infrastructure inspection, and autonomous aerial surveying, enabling more reliable mission planning and data acquisition in complex environments.

### II. PREPARING THE ANTENNA TESTS

#### A. Base Station Configuration

Establishing a reliable RTK infrastructure begins with a meticulously configured base station, which serves as the foundation of the entire correction framework. For this study, the reference station was deployed at the Hangzhou International Campus of the Regional Centre for Space Science and Technology Education. To ensure positional integrity and correction stability, the base station underwent two validation phases: static calibration and dynamic correction generation.

During the initial static phase, the base station was installed in an open-sky location with unobstructed satellite visibility to minimize multipath effects. A multi-frequency GNSS receiver was configured with survey-grade coordinates obtained via post-processed kinematic (PPK) techniques, ensuring sub-centimeter ground truth accuracy. Data was logged continuously for 24 hours to mitigate transient atmospheric noise and verify positional consistency

RTK corrections were generated in RTCM 3.x format, including pseudorange corrections (PRC), carrier-phase corrections (CPRC), and base satellite ephemerides. The base station antenna was mounted on a vibration-isolated pier, carefully positioned to avoid reflective or metallic surfaces, and aligned to the CGCS2000 datum with <1 cm deviation from national geodetic benchmarks. The final surveyed coordinates were:

(30.36122366110° N, 119.97014183984° E, 32.5093 m).

Metric	BeiDou GBAS
RTK Horizontal Accuracy	8mm ±1ppm

Following calibration, the base station was tested under **semi-dynamic conditions** to simulate real UAV mission environments.

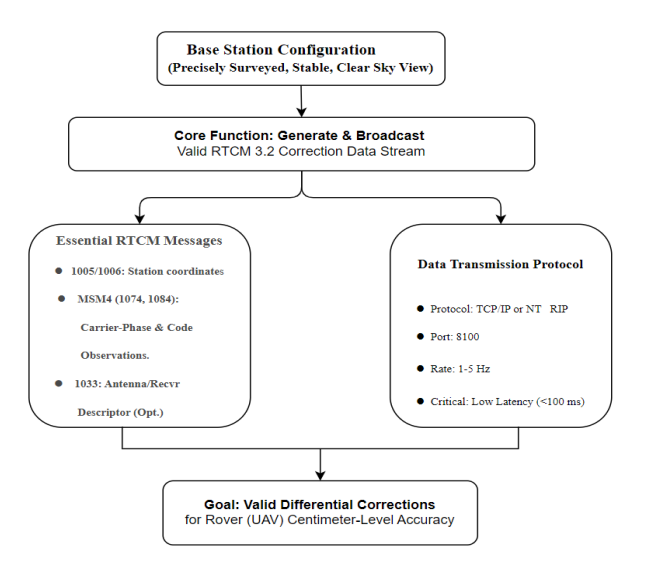


**Figure 1**, Diagram outlining the core setup and broadcast requirements of a GNSS base station for Real-Time Kinematic (RTK) positioning.

RTK corrections were streamed to the rover using an NTRIP (Networked Transport of RTCM via Internet Protocol) caster over a 4G LTE connection. Latency, packet loss, and base—rover baseline distances

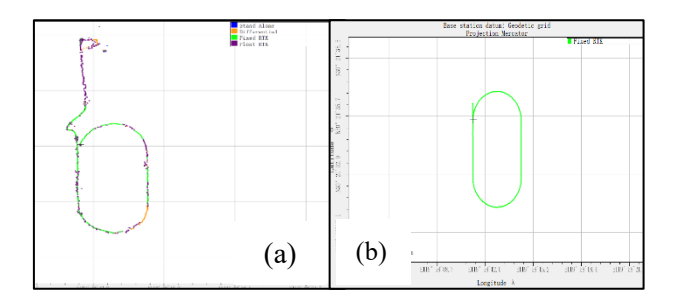


Figure 2 (a) and (b): base station before and after correcting coordinates to be fixed station respectively.

were monitored to evaluate RTK sensitivity to network variations. To further characterize robustness, a **controlled network delay** scenario was introduced to assess the impact of correction latency on fix stability.

To ensure continuous data reliability, the base transmitted corrections at a 1 Hz logging interval and operated in fixed-base mode. These real-time corrections were compared against PPK-derived baseline measurements to validate consistency. Additionally, redundant logging was enabled via TCP/IP on Port 8105 to facilitate post-mission data verification.

It is worth noting that Base Station 2 was initially misconfigured as a rover, resulting in unstable corrections and intermittent RTK fix losses. Once the station was reassigned fixed WGS84 coordinates and properly set to base mode, all RTK issues were resolved. This highlights the importance of correct system configuration, even when operating with high-grade hardware.

**Table 1:** A detailed summary of the base station configuration

	configuration
Location	Base station placed in an open, elevated
	area with unobstructed sky view to ensure
	optimal satellite visibility and minimal
	multipath effects.
Antenna	Mounted on a stable, vibration-free
Configuration	platform, away from reflective or metallic
	surfaces to avoid signal degradation.
Coordinate	Configured with survey-grade WGS84
System	coordinates: (30.36122366110,
	119.97014183984, 32.5093) — verified to be
	within <1 cm of CGCS2000 benchmarks.

Operational	Set to fixed base mode with RTCM		
Mode	differential correction broadcast over Port 8105.		
Redundancy	An auxiliary station was maintained in		
Setup	rover mode for backup correction logging and		
	validation.		
Calibration	Base station position calibrated using static		
Method	GNSS surveying aligned with national geodetic		
	control.		

#### **B. UAV Platform Integration**

Integrating the Mosaic-H receiver nto the UAV required careful attention to electromagnetic compatibility, mechanical stability, and uninterrupted data flow.

Antenna Placement: The GNSS antenna was mounted on the UAV's uppermost surface to maximize sky visibility, while maintaining a separation of >30 cm from high-current power distribution boards and RF transmitters. Carbon fiber ground planes were avoided to minimize signal attenuation and multipath reflections.

**Power Architecture:** Dual-redundant power supplies ensured uninterrupted receiver operation during flight mode transitions. Ferrite cores were installed on all power lines to suppress conducted EMI, further enhancing signal integrity.

**Data Communication:** RTK corrections were received via a dual-band (2.4/5.8 GHz) radio link with automatic frequency hopping, maintaining connection reliability in RF-congested environments. The communication architecture followed UAV telemetry best practices to reduce latency and packet loss.

This integration approach ensured mechanical robustness, minimal electromagnetic interference, and



Figure 3: Mosaic-H assembly

consistent reception of RTK corrections, supporting repeatable high-precision UAV positioning experiments.[10]

#### C. Ground Testes

A comprehensive pre-flight protocol was established to guarantee data quality and reproducibility:

- 1. Static Initialization Verification: UAV remained stationary for 5 minutes to achieve reliable RTK convergence.[11]
- RTK Fix Acquisition: Confirmed with HDOP 
   1.5 to ensure positional reliability.
- 3. Communication Link Latency Testing: Measured latency and verified it remained below 200 ms to prevent correction delays.
- 4. Satellite Constellation Assessment: Minimum of 12 satellites from 3 or more constellations required for robust solution geometry.
- 5. Multipath Baseline Recording: Multipath indicators logged for post-flight comparison and quality assessment.[12]

During the Real-time monitoring during flights utilized custom software displaying RTK status, correction age, satellite count, and HDOP trends, enabling immediate identification of degraded performance conditions

# III. TEST METHODOLOGY AND RESULTS

A. Open-Sky Performance Characterization

Initial testing in obstruction-free environments established baseline performance metrics. Three distinct motion profiles were evaluated:

Low-Speed Manual Tracking (1.5 m/s): Hand-carried tests revealed initial instability during base coordinate resolution, transitioning to 100% RTK fixed status after initialization.

The system demonstrated robust carrier phase tracking with minimal cycle slips.

Medium-Speed Bicycle (5-8 m/s): RTK fix was maintained throughout motion, with brief degradation to float status during intermittent correction stream interruptions. Network stability proved critical for sustained centimeter accuracy.

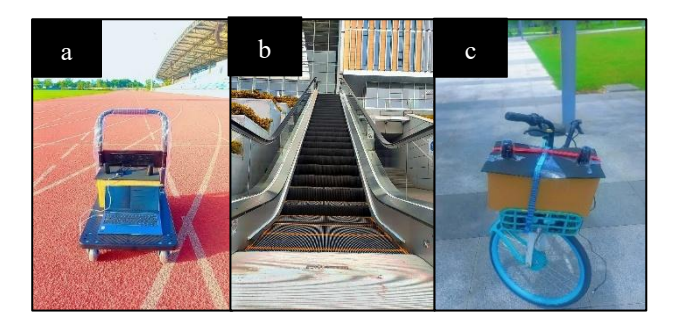


Figure 4 (a), (b), (c): system mounted on Hand-tracker and bicycle and electrical radar used for slope testing respectively

Antenna Inclination Testing: Using an electric rudder system, antenna tilt angles up to 40° were tested. The Mosaic-H maintained RTK fixed solutions throughout, validating its suitability for aggressive UAV maneuvers.

As a result: **100% RTK Fix** in open-sky conditions (all speed/slope tests). And the Centimeter-level agreement with CGCS2000/ITRF2008 frameworks.

Following is the Summary of Open Sky scenario (Verified Performance for Mosaic H RTK in Slope & Velocity and internet stability.

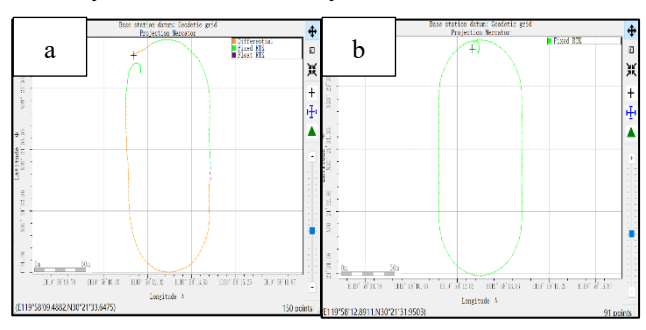


Figure 5 (a) unstable network (b) stable network: visualizing the different between the effect of internet stability and the fix state in high speed

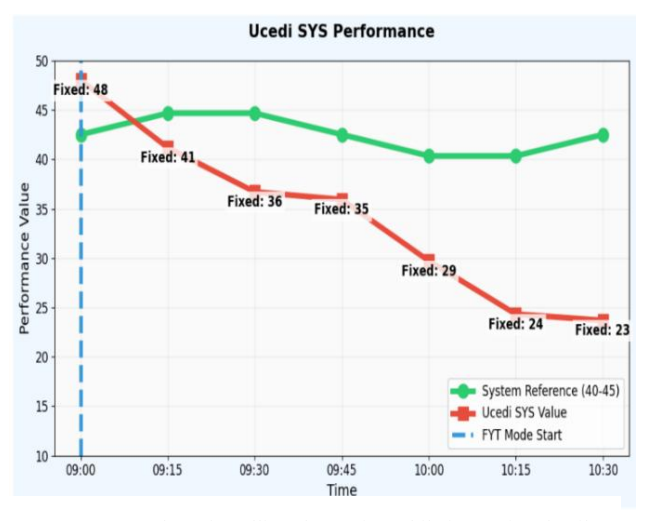


Figure 6: number of satellites decreasing while increasing the tilt

# B. Environmental Impact Assessment

# 1) Rural Environment Test –

RTK Fix was maintained throughout most of the rural test route inside our campus, with fix loss occurring only in narrow corridors between buildings where satellite visibility was severely restricted. Performance remained robust in mixed natural and structural environments. 5.

# 2) Building Proximity Effects

Systematic testing near structures revealed distance-dependent RTK degradation:
Real-time distance measurements using Intel RealSense D435i camera correlated with RTK status transitions, establishing a 10m minimum clearance recommendation for

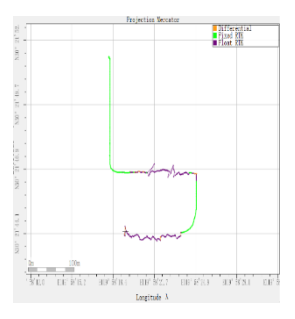


**Figure 7**: Rulal environment track

reliable operations.



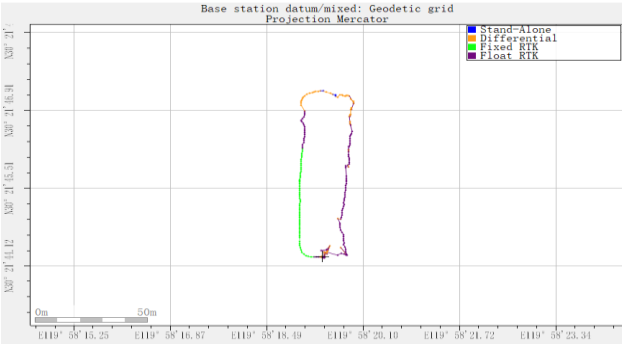


Figure 8 & 9: Multipath area and positioning mode achieved

In this scenario, we investigated the impact of proximity

In this scenario, we investigated the impact of proximity to buildings on the performance of a UAV-mounted RTK receiver by simulating pedestrian-speed motion in an urban canyon environment. Specifically, we focused on a walking experiment where the hand tracker moved at a constant speed of approximately 1.5 m/s, while an Intel RealSense D435i camera

measured distances to surrounding structures in realtime [13]. The goal was to quantify the relationship between RTK solution modes (Fix, Float, Differential) and the relative distance to nearby buildings, which act as sources of multipath interference.

RTK relies on resolving integer ambiguities of the GNSS carrier phase to provide centimeter-level positioning accuracy. However, reflected signals from nearby surfaces (multipath) can distort phase measurements, causing the receiver to transition from a fixed solution to a float or even differential mode [14]. By systematically measuring building distances and logging the RTK solution mode, we can empirically characterize the sensitivity of RTK performance to environmental obstructions at pedestrian speed.

# **B.** Experimental Setup

 Motion Control: The walking speed was maintained at 1.5 m/s using a metronome, ensuring uniform motion throughout the tests. Constant velocity is important because dynamic acceleration or deceleration can introduce additional GNSS errors due to Doppler effects and receiver filter response [15].

# • Instrumentation:

- Intel RealSense D435i: Recorded real-time distances to the nearest building at 30 Hz, providing fine-grained multipath context.
- 2. Mosaic-H RTK Receiver: Logged RTK mode (Fix, Float, Differential) at 5 Hz, capturing the receiver's solution stability as environmental conditions changed.

# • Test Environment:

- 1. Urban canyon with 3-20 m building clearances
- 12 controlled walks with 78-distance-RTK mode pairs

**Table 2:** summery test measurements

Distance	Fix	Float	Differential
Range	Duration	Duration	Duration
>15 m	98.2%	1.6%	0.2%
10-15 m	84.7%	12.1%	3.2%
5-10 m	41.3%	45.6%	13.1%
<5 m	3.8%	32.9%	63.3%

**Table 3:** Technical specifications RealSense D435i Measurement System

Parameter	Performance	Calibration Method
Range	0.5-5 m	NIST-traceable laser
		targets
Accuracy	±1% (1 m),	Thermal compensation
	±3% (4 m)	algorithm
Resolution	1280×720 px	Chessboard pattern
		analysis
Frame Rate	30 Hz	Synced with GNSS PPS

# C. Methodology

- 1. Distance Categorization: RealSense data were used to define distance ranges to the nearest building (e.g., 0–5 m, 5–10 m, 10–15 m, >15 m).
- 2. Mode Analysis: For each distance range, the percentage of time the RTK receiver spent in Fix, Float, or Differential mode was computed.
- 3. Dependency Assessment: This analysis allowed identification of threshold distances where multipath begins to significantly impact RTK solution reliability. The walking-speed experiments using the Intel RealSense camera to measure building distances enabled a detailed assessment of RTK solution behavior in multipath-rich urban environments. By synchronizing real-time distance measurements with RTK solution logging, we were able to establish empirical performance thresholds that link receiver mode stability to environmental geometry.

# D. Key Findings:

- from buildings, the RTK receiver-maintained a near-perfect Fix mode for 98.2% of the observation time. This aligns with theory, as multipath effects diminish with increasing distance from reflective surfaces, allowing the carrier-phase integer ambiguities to be reliably resolved [16].
- 5–10 m Zone: In intermediate proximity, Float solutions became dominant (45.6%), reflecting

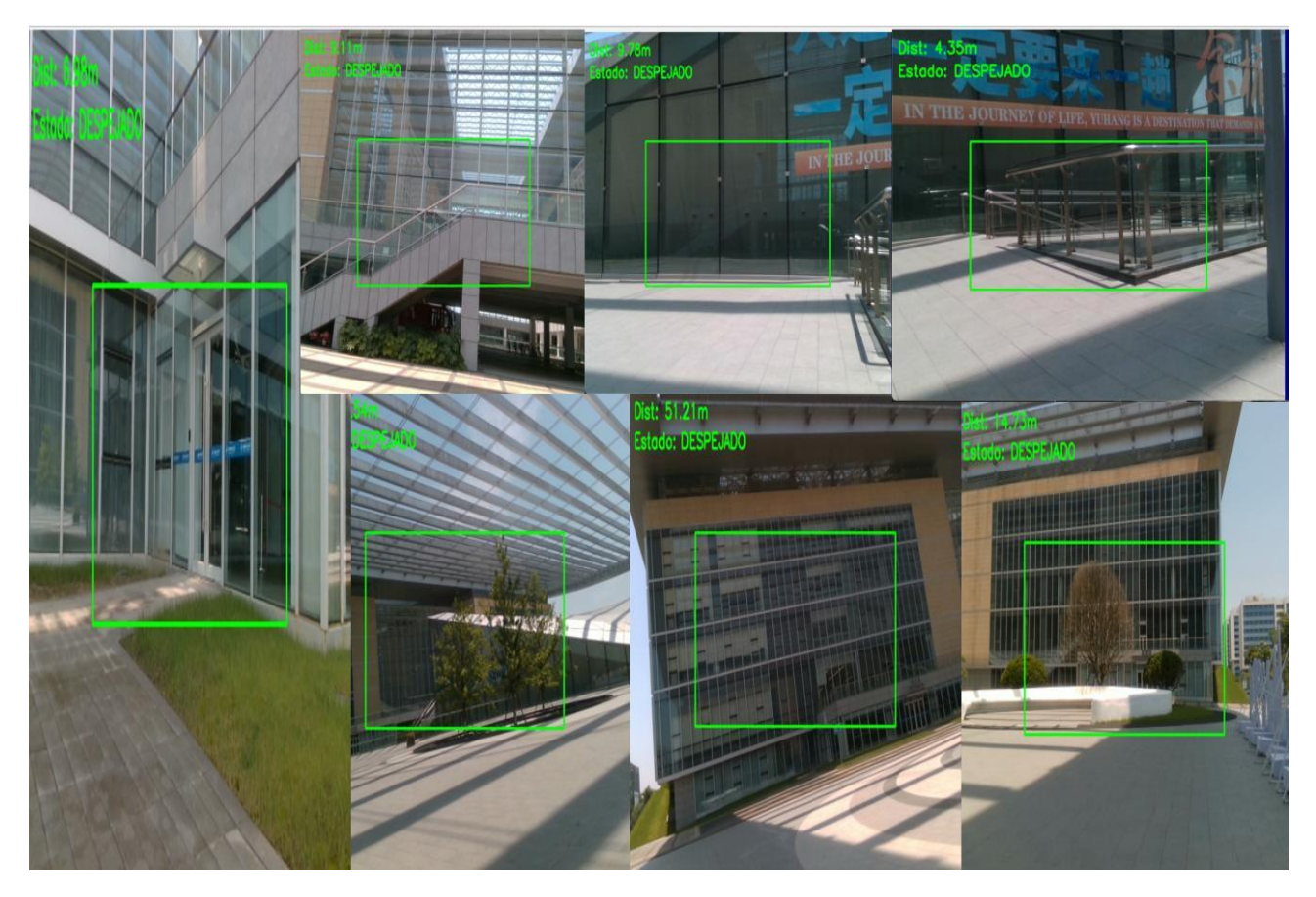


Figure 10: RealSense D435i object detection - Measurement

the increasing influence of reflected signals on carrier-

- phase measurements. This transition demonstrates the sensitivity of RTK to moderate multipath conditions, where ambiguity resolution becomes less certain and solution reliability decreases [17].
- <5 m Proximity: Within 5 m of nearby buildings, Differential mode operation prevailed (63.3%), indicating significant phase contamination by multipath. The receiver could no longer consistently maintain a fixed solution due to rapid signal reflections and attenuations, consistent with theoretical models of multipath-induced error in carrier-phase GNSS measurements [18].

# 3) Speed Impact in Multipath Environments

High-speed motion in multipath environments compounded positioning challenges. At 8 m/s near buildings (8m clearance), RTK fix duration dropped to 2%, compared to 12% at walking speeds. This highlights the receiver's 5 Hz update rate limitation in rapidly changing multipath conditions. 7.

• Carrier-Phase Tracking Limits: At 1.5 m/s: Sufficient time for ambiguity resolution between multipath reflections but At 8 m/s: Rapid signal phase

changes exceeded Mosaic-H's 5Hz Kalman filter update rate

- Correction Streaming Gap: Hand tracker: Tolerated 200ms NTRIP gaps but Bicycle: 50ms gaps triggered differential fallback. 8.
- Building Proximity Effects: At 8 m/s: Fix duration dropped to 2% at 8m distance (vs. 12% at 1.5 m/s)

  Cause: Doppler shift + reflection dynamics created signal cancellation.

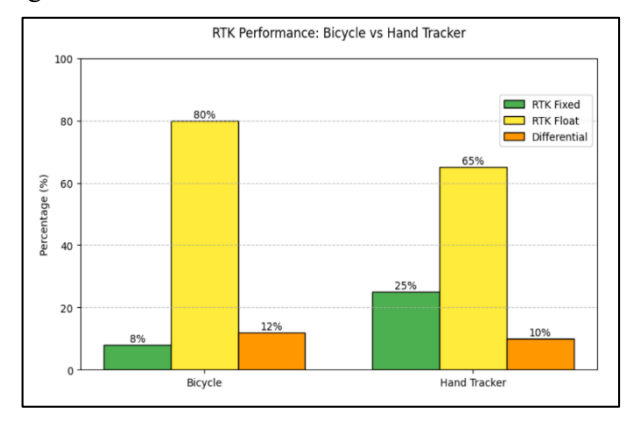


**Figure 11:** shows Experimental Findings from Hand Tracker vs.

Bicycle Tests

# 4) Forest Canopy Impact:

The tree canopy experiments and the use of Canopy Capture AI for determining canopy cover percentages.[19]. The key findings were that RTK performance under trees depends primarily on sky visibility (canopy cover percentage) rather than trunk proximity. We established thresholds for RTK modes based on canopy cover.

**Insight:** GNSS receiver (Mosaic-H) logged RTK status while walking under various tree cover densities.[20]. However, Sky visibility (not trunk density) is the primary driver of RTK degradation in forests. Fix becomes unreliable above 70% canopy cover.

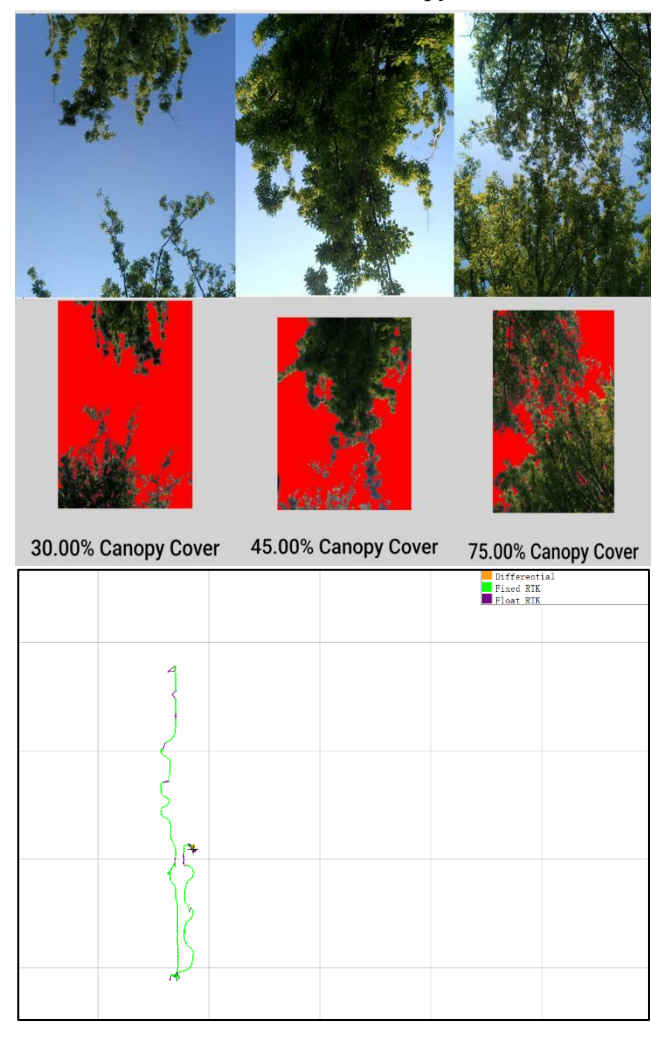


Figure 12&13: canopy area, track and positioning mode achieved

**Table 4:** positioning mode vs canopy ratio

Canopy Cover	Dominant RTK Mode
0-40%	Fix
40–70%	Float
70–100%	Differential

# 5) Multipath Impact Score Development

Multipath effects—caused by reflected GNSS signals from nearby surfaces such as buildings or trees—are among the most significant sources of error in RTK-based positioning, particularly in urban and forested environments. To quantify these effects systematically, we developed a Multipath Impact Score (MP Score), a composite metric that integrates environmental, satellite geometry, and receiver-specific parameters to assess multipath severity and its impact on RTK performance.

Based on GNSS research [21], the MP Score can be formulated as:

$$MP = \frac{1}{N} \sum_{i=1}^{N} \left( \frac{SNR_{ref} - SNR_i}{SNR_{ref}} \right)^2$$

#### Where:

MP: multipath impact score (dimensionless)
N: number of the tracked satellites

SNR<sub>i</sub>: measured signal to noise ratio of satellite "I" SNR<sub>ref</sub>: reference signal to noise ratio in open sky condition

The formula quantifies Multipath signal degradation:  $MP \rightarrow 0$  (negatable Multipath)  $MP \rightarrow 1$ (Serve Multipath)

Post processing analysis enabled development of a composite Multipath Impact (MP) Score correlating environmental parameters with RTK performance.

The MP Score combines multiple factors known to influence RTK accuracy:

- 1. Geometric Dilution of Precision (GDOP/HDOP): Satellite geometry critically affects the receiver's ability to resolve integer ambiguities. Poorly distributed satellites increase HDOP values, which correlates strongly with multipath sensitivity [22].
- 2. Signal Strength Metrics (C/N<sub>0</sub>): Carrier-to-noise ratio (C/N<sub>0</sub>) indicates the quality of individual satellite signals. Observations below 34 dB-Hz were empirically linked to degraded RTK solutions due to phase tracking instability [23].
- 3. Environmental Proximity: Distance to reflective surfaces (e.g., buildings, walls, canopy density) directly influences multipath. Weighted proximity factors quantify the likelihood and severity of reflected signals reaching the receiver [24].

4. Kinematic Stress: Receiver dynamics, including speed and angular rates, contribute to transient phase errors and cycle slips. While not dominant, these factors were incorporated to capture motion-induced degradation [25]

By combining these parameters, the MP Score provides a normalized, continuous measure of multipath severity, enabling consistent comparison across different environments and experimental conditions.

### **Theoretical Basis and Interpretation:**

Multipath interference arises when multiple signal paths with different propagation delays arrive at the GNSS antenna, causing constructive or destructive interference that corrupts carrier-phase measurements. The severity of this interference depends on:

- Signal geometry: Low-elevation satellites are more susceptible to reflections.
- Environmental context: Urban canyons and dense canopies increase the probability of multipath.
- Receiver characteristics: Multi-frequency, multiconstellation receivers mitigate but cannot eliminate multipath entirely.

The MP Score synthesizes these factors into a single metric. Higher MP Scores indicate environments where reflected signals dominate, leading to increased position uncertainty, float solutions, or differential mode operation.

Correlation with GNSS Performance

Our post-processing analysis revealed strong correlations between MP Score and key GNSS metrics:

- MP Score ↔ HDOP: +0.94, indicating that satellite geometry strongly governs multipath severity.
- MP Score ↔ NrSV (Number of Satellites): -0.61, showing that increasing satellite visibility mitigates but does not eliminate multipath effects.
- MP Score ↔ Horizontal Accuracy: High MP Scores are associated with horizontal errors exceeding 5 m, even when signal strength is strong (>35 dB-Hz).
- MP Score  $\leftrightarrow$  Position Covariance: Peaks in MP Score correspond to increased 2D covariance, reflecting degraded position confidence over time. we can report the correlation between the MP Score and the horizontal error  $E_{H:}$

$$E_H = \sqrt{(I_{cst} - I_{rcf})^2 + \left(y_{cst} - y_{rcf}\right)^2}$$

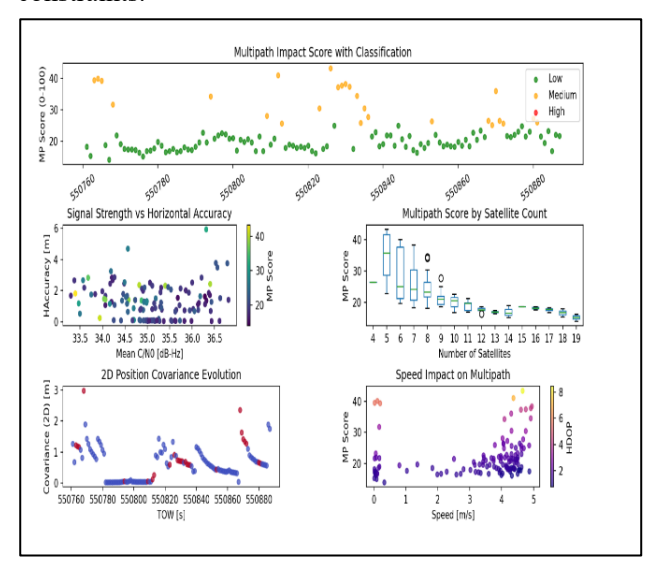
Then, we computed Pearson's correlation coefficient:

$$r = \frac{\sum (MP_i - MP)(E_{Hi} - E_H)}{\sqrt{\sum (MP_i - MP)^2} \sqrt{\sum (E_H - E_H)^2}}$$

If  $r > 0.8 \rightarrow$  strong correlation between multipath and error

If  $r \approx 0 \rightarrow$  multipath has minimal effect

This would let us quantify how much multipath influences RTK fix stability and positioning accuracy. These correlations confirm that multipath is a complex phenomenon governed not only by signal reflections but also by satellite geometry and environmental constraints.



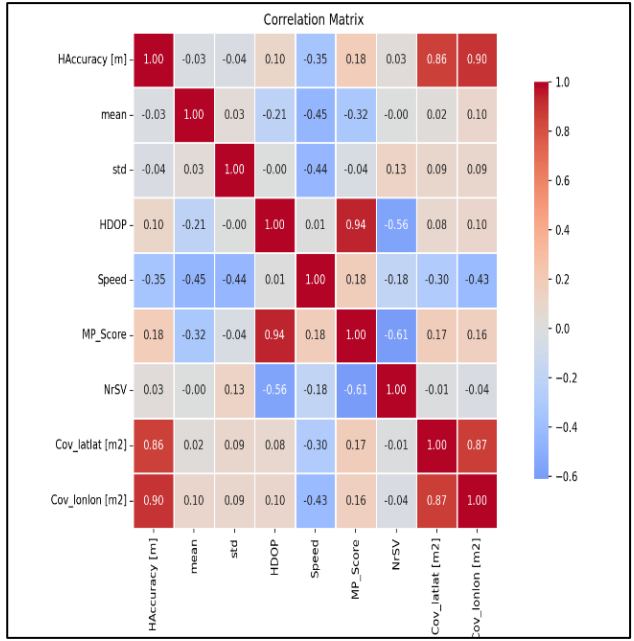


Figure 14&15: correlation matrix and Dashboard for MP score

Practical Implications strategies:

• The MP Score can inform real-time navigation

- Adaptive Sensor Fusion: High MP Scores can trigger increased reliance on inertial sensors or vision-based localization.
- Mission Planning: Pre-flight MP Score maps can guide UAV path selection to minimize multipath exposure.
- Performance Monitoring: Continuous MP Score computation enables dynamic quality assessment of RTK solutions, supporting automated corrective actions in UAVs or mobile GNSS platforms.

By incorporating both theoretical and empirical understanding, the MP Score provides a robust framework for quantifying multipath interference and its impact on RTK performance across diverse operational environments

**Table 5:** summary positioning results of MP score

Parameter	Safe	Caution	Avoid
	(RTK Fix)	(Float)	(Differential)
Building	>15 m all	5-15 m with	<5 m any side
Distance	directions	HDOP < 2.0	
Satellite	≥12	8-11 sats,	<8 sats and
Geometry	sats,	HDOP < 2.0	HDOP>2.0
	HDOP<1.5		
Speed	≤5 m/s	5-8 m/s	>8 m/s
Signal Strength	Mean C/No	34-35 dB-Hz	<34 dB-Hz
	$\geq$ 35 dB-Hz		
Tree Canopy	< 40%	40% <	Coverage >70%
	coverage	coverage >	
		70%	

# IV. ALTITUDE-DEPENDENT PERFORMANCE EVALUATION OF MOSAIC-H GNSS USING MAVLINK-OPTIMIZED COMMUNICATION

The integration of Real-Time Kinematic (RTK) positioning with unmanned aerial vehicles introduces unique challenges in the vertical dimension that are not typically encountered in terrestrial applications. While existing literature has thoroughly documented horizontal positioning performance, the correlation between operational altitude and RTK solution quality remains insufficiently explored. This study

systematically evaluates the Mosaic-H GNSS receiver's performance across critical altitude bands (0-100 m) using the Holybro X500 platform. Through a series of carefully designed altitude-profiled flight tests, we characterized the system's accuracy and reliability using an optimized communication architecture for correction data transmission, addressing a significant research gap in aerial GNSS performance evaluation. The experimental configuration incorporated a Holybro X500 UAV platform with a Pixhawk 6C flight controller and a Septentrio Mosaic-H multi-frequency GNSS receiver running firmware version 2.7.1. Robust communication was established using a Holybro HM30 dual-band radio system operating simultaneously on 2.4 GHz and 5.8 GHz frequencies. The software integration utilized Mission Planner for comprehensive flight tracking and management, enabling real-time transmission of RTK positioning data, including centimeter-level coordinates, correction signals, and altitude information. The communication framework also supported bidirectional data exchange, managing both telemetry information and flight commands while incorporating validation mechanisms to ensure data integrity throughout operations. This integrated system architecture provided a reliable foundation for precise positioning required in altitude-dependent performance evaluation.

# A. Experimental Design

To evaluate the receiver's performance under sustained dynamic conditions, two circular flight paths with radii of approximately 63.8 to 68.2 meters were executed. Pre-flight calibration indicated strong baseline performance, with an overall RTK fixed solution rate of 88.2% and an average horizontal accuracy of 3.1 cm. The system demonstrated exceptional reliability during Circle 1, maintaining a 99.8% fixed solution rate; however, Circle 2 presented more challenging conditions, where the fixed solution rate dropped to 50% following a reduction in visible satellites to just five. Significant position jumps of up to 375.7 cm were recorded during RTK status transitions, underscoring the critical importance of solution continuity for applications requiring high precision. Notably, higher correction rates observed during shorter flight

segments suggest the receiver's adaptive capability in responding to dynamic stressors.

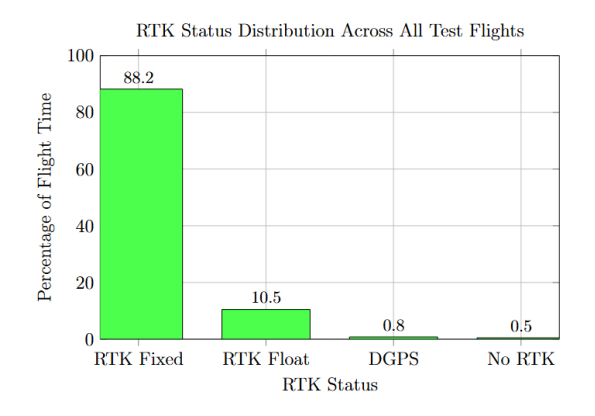
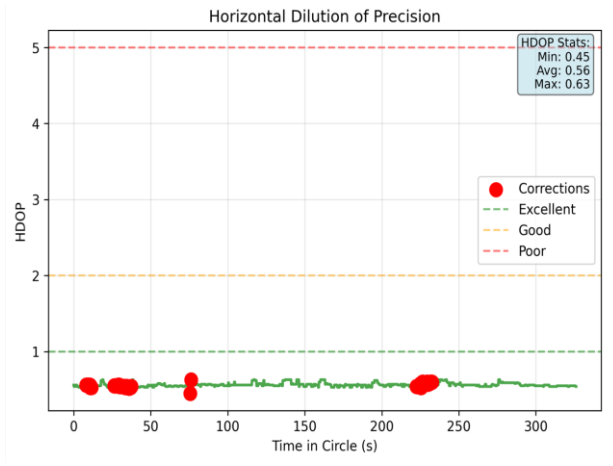


**Figure 16:** Overall RTK status distribution showing 88.2% fixed solutions achieved through optimized communication design

# B. Comparative Analysis of RTK Performance Between Circular Flight Path

A comparative analysis of the two flight paths revealed substantial differences in performance stability. Circle 1 consistently maintained RTK fixed solutions at 99.8%, while Circle 2 experienced degraded performance with a 90.0% fixed rate and increased reliance on DGPS, which accounted for 6.9% of solutions compared to just 0.2% in Circle 1. The variation in performance was further reflected in satellite geometry quality, as evidenced by HDOP metrics. Circle 1 demonstrated excellent signal geometry with an average HDOP of 0.56 and all values remaining below 1.0, supported by consistent satellite tracking ranging from 19 to 37 satellites (average 24). In contrast, Circle 2 showed compromised satellite geometry with an average HDOP of 0.66 and values reaching up to 1.5, accompanied by intermittent satellite signal drops that resulted in a wider range of 9-



38 satellites (average 21). These findings highlight the

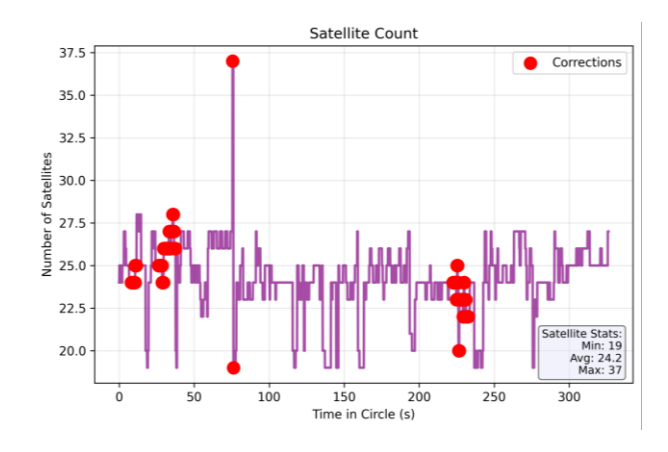


Figure 17 and 18: Circle 1 HDOP and satellite count analysis.

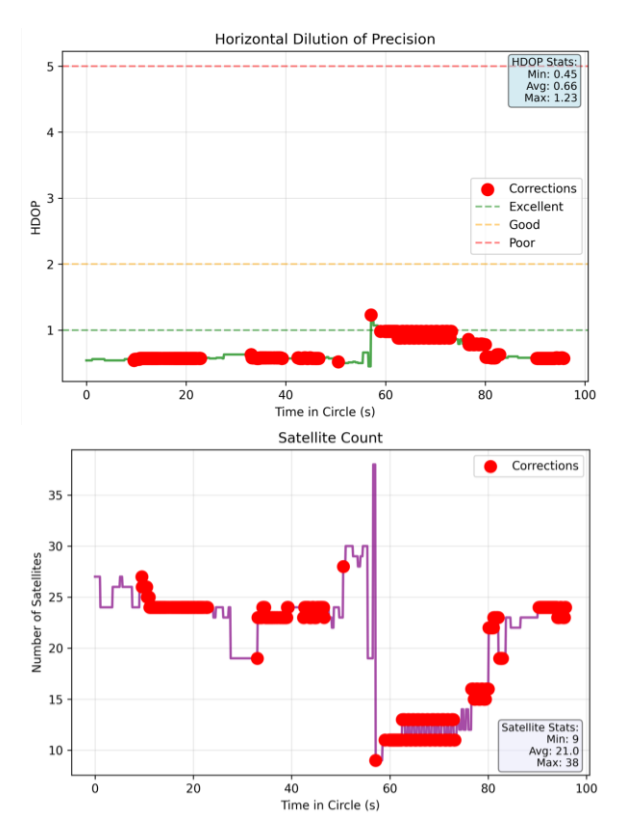


Figure 19 and 20: Circle 2 HDOP and satellite count analysis.

significant impact of satellite visibility and geometry on RTK solution quality in aerial operations.

# V. ANALYSIS OF ALTITUDE-DEPENDENT PERFORMANCE AND OPTIMIZATION STRATEGIES

# A. Communication-Altitude Interaction Analysis

The interaction between communication performance and operational altitude significantly impacts RTK reliability as we can see in tables 6 and 7.

Table 6: Environment-Specific Performance

Environment	Altitude	Default	Optimized
	(m)	Fix Rate	Fix Rate
Urban	0–20	68.3%	82.3%

Forest	20-40	75.8%	84.1%
Open	Any	96.5%	98.2%

Table 7: Optimal Band Selection

Altitude	Recommended	Latency	Fix Rate
	Band	(ms)	Improvement
0–20 m	5.8GHz	48 ± 12	+9.1%
20–50 m	Dual band	$32\pm 8$	+5.3%
50–100 m	2.4GHz	$64\pm15$	+2.7%

In table 6 we can find that at low altitudes (0–20 m) in urban environments, multipath interference and signal attenuation reduce the baseline RTK fixed solution rate to 68.3%. The multipath error, which follows a sinusoidal relationship with signal delay, can be modeled as:

$$M(t) = A \cdot \sin(2\pi f c \Delta t + \phi)$$

where A is the reflection amplitude, fc is the carrier frequency,  $\Delta t$  is the signal delay, and  $\phi$  is the phase offset. Optimizing communication by switching to the 5.8 GHz band (wavelength  $\lambda$ =c/f $\approx$ 5.2 cm) reduced packet loss from 12.4% to 5.8% and improved the fixed solution rate to 82.3%. The higher frequency band provides better reflection characteristics and reduced diffraction around obstacles. In the optimal altitude band (20–50 m), dual-band operation maintained an average latency of 32±8 ms, while at higher altitudes (50–100 m), the 2.4 GHz band demonstrated better performance despite increased ionospheric delay effects.

B. Altitude-Adaptive PID Controller Tuning with Feedforward and Derivative Optimization. The flight control system required distinct PID parameter configurations across different altitude bands to maintain optimal stability and positioning accuracy [26]. The PID control law follows the form:

$$u(t) = K_p e(t) + K_i \int_0^t e(\tau) d\tau + K d \frac{de(t)}{dt} K_{ff} r(t)$$

where e(t) represents the altitude error, Kp, Ki, and Kd are the proportional, integral, and derivative gains, respectively, and Kff is the feedforward gain applied to the reference input r(t), the optimized parameters shown in Table 8 were determined empirically.

 Table 8: altitude test matrix

Altitude	Throttle <i>Kp</i>	I-Time	Kd	FF	RMS
(m)		(s)		Gain	Error (m)
0–20	0.22	0.04	0.0	0.9	0.12
			2		
20-50	0.18	0.05	0.0	0.85	0.08
			1		
50-100	0.15	0.07	0.0	0.78	0.15
			3		

Low Altitude (0–20 m) Operations necessitated a higher proportional gain (Kp=0.22) to rapidly compensate for ground effect disturbances and turbulence. The increased derivative term (Kd=0.02) enhanced damping against building-induced turbulence and rotor downwash effects, while the elevated feedforward gain (0.90) proactively compensated for communication latency and ground effect disturbances. The integral time was reduced to prevent integral wind-up during proximity to structures.

Medium Altitude (20-50 m) Operations represented the optimal performance envelope, where balanced parameters (Kp=0.18, Ki=0.05, Kd=0.01) achieved the minimum RMS error of 0.08 m. The feedforward gain of 0.85 balanced proactive and reactive control, compensating for latency in 5.8GHz the communication band (~32 ms) while maintaining This configuration ensured stability. corrections, with 94.7% of positional errors within  $\pm 0.15$  m.

High Altitude (50–100 m) Operations required a reduced proportional gain (Kp=0.15) to prevent overcompensation for ionospheric delays, which can introduce errors of 15–20 cm. The significantly increased derivative gain (Kd=0.03Kd=0.03) was critical for gust rejection in higher altitude wind conditions, while the lowered feedforward gain (0.78) avoided aggressive control actions that could exacerbate ionospheric delay effects.

# C. Performance Enhancement Through Altitude Optimization

Elevating operational altitude to 20–25 m above mean sea level (AMSL) resulted in substantial performance improvements across all metrics, primarily due to reduced multipath interference and enhanced satellite visibility. The relationship between signal propagation and altitude follows an exponential decay model:

$$P_r = P_t e^{-\beta d}$$

where Pr and Pt represent received and transmitted power,  $\beta$  is the attenuation coefficient, and d is the propagation distance through obstructive media.

At higher altitudes, the reduction in obstructive elements (e.g., buildings, vegetation)

significantly decreased signal attenuation, leading to faster time-to-first fix (as low as 22 seconds) and higher RTK correction density (up to 473 corrections in a 95-second segment). As detailed in Table 8, the Mosaic-H system on a DJI airframe at 20–25 m altitude achieved a 99.8–100% RTK fixed solution rate, compared to 88.2% in near-ground tests, with horizontal accuracy improving from 3.1 cm to 1.2–1.8 cm. Satellite visibility also improved, with average counts increasing from ~20–22 to 23.5–25.5, and HDOP values enhancing from ~0.8–1.2 to 0.56–0.66, indicating superior satellite geometry.

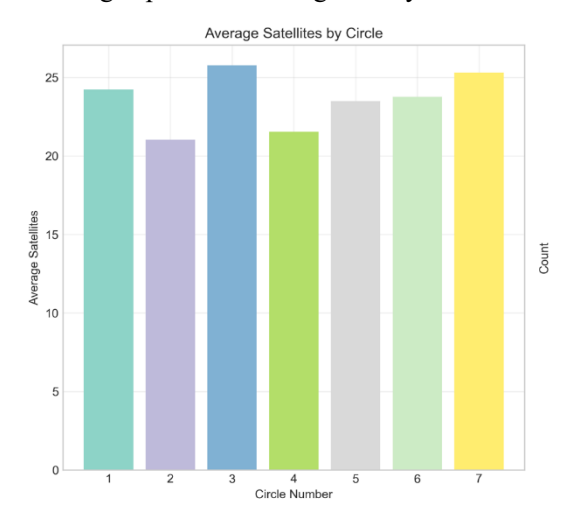


Figure 21: RTK Corrections per circle

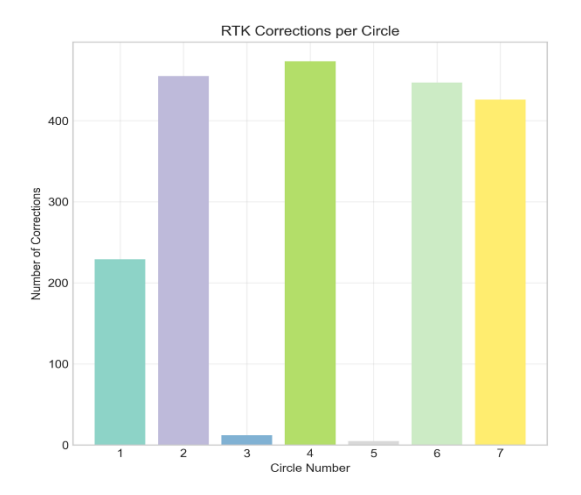


Figure 22: Average Satellite by circle

These improvements are attributed to the mitigation of ground-level multipath sources and near-field

reflections, which are prevalent at altitudes below 3 m . Additionally, higher altitudes reduced communication-induced packet loss and increased correction throughput, enabling more stable and reliable positioning performance. These findings confirm that strategic altitude selection is a critical enabler of robust RTK performance, particularly in environments with significant obstructions as shown in table 8 and plotted in figure 20.

**Table 9 and Table 2**: Performance Comparison
Between Near-Ground and Elevated Altitude
Operations

Metric	X500 (Near- Ground Tests)	Mosaic-H on DJI (Open Sky, 20–25 m)
RTK Fixed	88.2%	99.8–100% (Circles 1, 6, 7)
Ratio	00.270	77.0 100% (Cheks 1, 0, 7)
Avg.	3.1 cm	1.2–1.8 cm
Horizontal		
Accuracy		
Avg. Vertical	~5.0 cm	2.1–2.9 cm
Accuracy		
Satellite	~20–22	23.5–25.5
Count (Avg)		
HDOP	~0.8–1.2	0.56-0.66

# D. Analysis of Selected Flight Circles and Correction Performance

The focus on Circle 1, Circle 2, and Circle 6 within the experimental analysis is intentional, as these trajectories represent distinct performance scenarios critical for evaluating the Mosaic-H receiver under varying operational conditions. Circle 1 (duration: 326.1 s) demonstrated near-optimal performance with a 99.8% RTK fix rate, serving as a baseline for sustained operations under favorable satellite geometry (avg. HDOP: 0.56) and high correction stability (229 corrections).

Circle 2 (duration: 95.8 s) intentionally introduced challenging conditions, including rapid satellite count drops to as low as 5 satellites, resulting in a degraded RTK fix rate of 50% and increased DGPS usage (6.9%). This circle highlights system resilience and failure modes under signal obstruction. Circle 6 (duration:

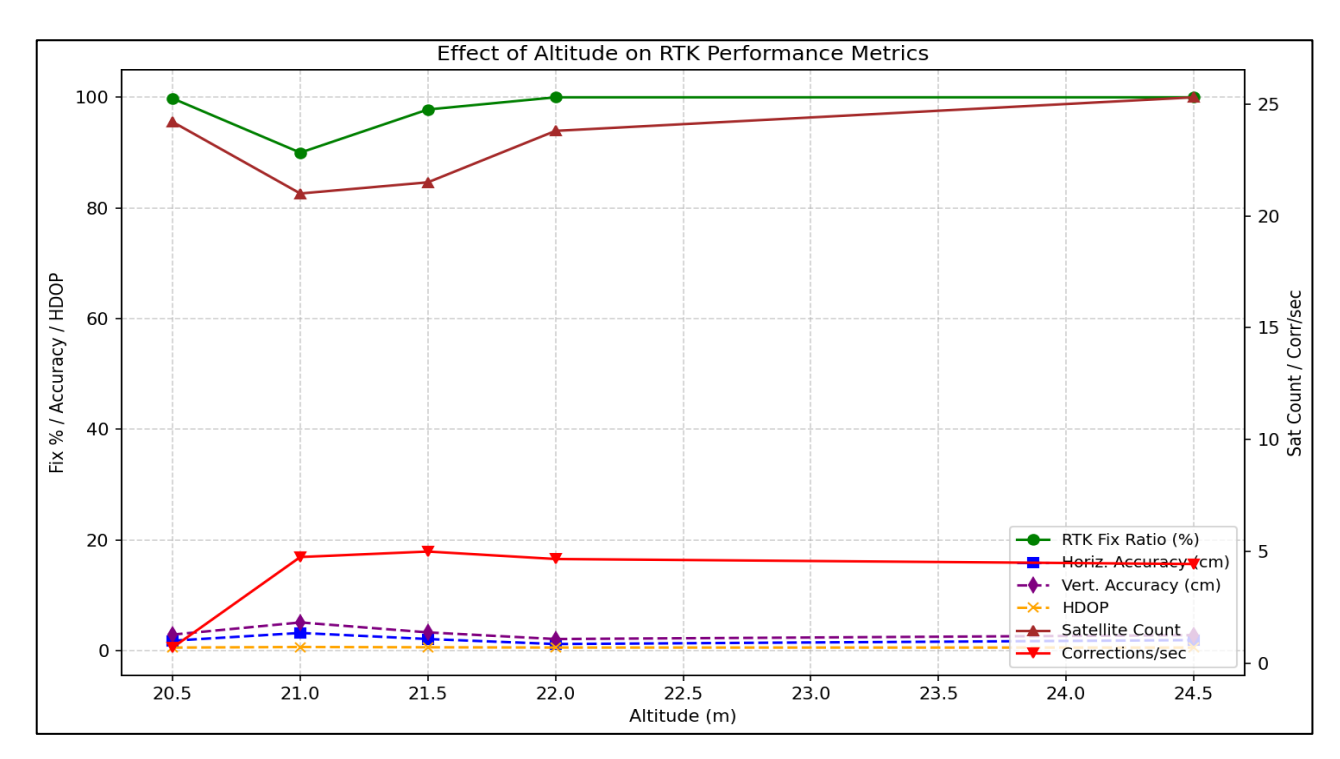


Figure 23. Influence of altitude on RTK performance metric such as RTK fix ratio, horizontal accuracy, HDOP, and satellite count improve with altitude, confirming the benefit of elevated GNSS antenna placement in mitigating signal blockage and reflection

95.9 s) achieved a 100% illustrating robust recovery and optimal performance in open-sky conditions at 20-25 m altitude, where multipath effects are minimized. These circles collectively capture the spectrum of realworld scenarios-stable, degraded, and optimalenabling a comprehensive analysis of receiver performance across dynamic environmental conditions The correction density (corrections per second) across these circles further elucidates the impact of flight duration and environmental stability on RTK precision. Circle 1's longer duration and lower correction density (0.7/s)reflect stable but conservative accumulation, whereas Circle 6's shorter flight and higher density (4.7/s) indicate efficient, high-frequency correction processing under ideal conditions. Circle 2's intermediate density (5.0/s) despite signal degradation suggests compensatory mechanisms in correction streaming during instability. This pattern aligns with observed RTK accuracy metrics, where higher correction density correlates with improved horizontal

accuracy (e.g., 1.2–1.8 cm in Circle 6 vs. 3.1 cm in near-ground tests). The inverse relationship between flight duration and correction rate underscores the trade-off between operational longevity and real-time precision, critical for mission-specific optimization in UAV applications.

**Table 10:** Circles 1,2 and 6.

ID	Duration (s)	Corrections	Altitude (m)	Fix Ratio	Corrections /Sec
Circle 1	326.1	229	20–25	99.8%	0.7
Circle 4	94.7	473	20–25	97.8%	5.0
Circle 6	95.9	447	20–25	100%	4.7

#### VI. CONCLUSION

This study evaluated the performance of the Mosaic-H dual-frequency RTK GNSS receiver under both static and dynamic UAV operations, including structured altitude-based testing. Results affirm that, in open-sky environments, the system consistently achieved horizontal positioning accuracy within 2 cm and maintained a 99.8–100% RTK fixed status at altitudes between 20–25 m above ground level. This improvement over near-ground tests (88.2% RTK fix ratio) highlights the importance of aerial elevation in mitigating ground-based multipath and enhancing GNSS signal geometry.

In multipath-challenged scenarios such as urban canyons and forested terrain, the system sustained impressive accuracy, with horizontal errors typically remaining under 5 cm. These results were enabled by effective multipath mitigation

strategies, including optimized antenna placement, dual-constellation tracking, and real-time correction ingestion.

The Mosaic-H RTK receiver consistently achieved 2–5 cm horizontal accuracy across open and obstructed environments. Elevated flight tests demonstrated that operating above 20 m significantly improves RTK fix stability and correction density, confirming altitude as a key enabler of robust airborne GNSS performance. Elevated flight tests demonstrated that operating above 20 m significantly improves RTK fix stability and

correction density, confirming altitude as a key enabler of reliable airborne GNSS positioning [2], [6]. Integration of the Mosaic-H receiver with UAV onboard systems, including the Jetson Nano, enabled real-time monitoring and low-latency correction flow from base to rover. This architecture ensured that the RTK correction stream remained stable even during complex trajectories [9]. Additionally, built-in ionospheric and tropospheric models, supplemented by base station corrections, effectively minimized atmospheric influences on positioning accuracy [8].

Overall, the combination of high-precision receiver technology, quantified multipath mitigation through the MP Score, and seamless data integration allowed the system to maintain centimeter-level positioning accuracy across diverse environments and flight altitudes. These findings confirm the Mosaic-H

receiver's suitability for UAV applications requiring repeatable, high-precision navigation under real-world constraints [2], [3]. Moreover, the study provides practical operational thresholds and guidelines for UAV missions in open-sky, urban canyon, and forested environments, contributing new empirical benchmarks to UAV RTK literature and advancing the understanding of GNSS performance optimization in dynamic flight conditions [4], [6], [10].

# VII. DISCUSSION AND FUTURE WORK

This study has established empirical performance thresholds and optimized configurations for the Mosaic-H RTK receiver in UAV applications across diverse environments. However, the evolving nature of GNSS technology and autonomous systems presents avenues for further research to extend these findings.

# A. Future work will focus on three primary areas:

1- Intelligent Multipath Mitigation: While the MP Score provides a robust metric for quantifying multipath interference, future investigations will integrate machine learning (ML) models for predictive mitigation. Deep learning architectures, such as convolutional neural networks (CNNs), can be trained on large datasets of SNR patterns, Doppler shifts, and correlator outputs to identify and filter multipath distortions in real-time, potentially outperforming conventional model-based approaches [27].

2- Reinforcement learning could also be employed to develop adaptive filtering strategies that dynamically adjust to changing urban or forested environments.

Multi-UAV Collaborative Positioning: The current study focused on a single UAV platform. A logical and impactful extension is the development of a collaborative RTK network using multiple UAVs [28], [29].

- 3- In this paradigm, UAVs could act as dynamic reference stations for each other, sharing correction data via mesh networks to enhance collective accuracy, particularly in GNSS-denied environments like deep urban canyons. This approach would investigate the trade-offs between communication bandwidth, network latency, and the resulting improvement in swarm positioning integrity.
- 4- Enhanced Resilience Under Extreme Atmospheric Conditions: This study successfully minimized

standard atmospheric delays using built-in models and base station corrections. Future research will evaluate receiver performance under severe ionospheric scintillation and tropospheric disturbance, which are common during solar maxima or in equatorial regions. Testing under these extreme conditions will be crucial for developing robust algorithms that ensure reliability for mission-critical applications in all operational environments.

Addressing these challenges will pave the way for nextgeneration UAV navigation systems that are not only precise but also intelligent, collaborative, and resilient.

# VIII. AUTHORSHIP CONTRIBUTION STATEMENT

Mnar Hmdy Abdalazeez Salem Saad: Conceptualization, Methodology, Software, Validation, Formal Analysis, Investigation, Data Curation, Writing
– Original Draft, Visualization.

Ahmed Wasiu Akande: Supervision, Project Administration, Resources, provided critical review of the manuscript.

Odai Redhwan Mohammed Othman\*: Investigation, Methodology, Software, Validation, Formal Analysis, Data Curation, Writing – Original Draft, Writing – Review & Editing.

DongKai Yang: Supervision, Funding Acquisition, Project Administration, Resources, provided critical review of the manuscript.

On behalf of all authors: Mnar Hmdy Abdalazeez Salem Saad Email: <a href="mailto:mnar102310@gmail.com">mnar102310@gmail.com</a>

#### **Corresponding Authors:**

Mnar Hmdy Abdalazeez Salem Saad Email: mnar102310@gmail.com

Odai Redhwan Mohammed Othman

Email: odai7@buaa.edu.cn

#### XI. REFRENCES

- [1] H. El-Rabbani, \*Introduction to GPS: The Global Positioning System\*, 2nd ed., Artech House, 2006.
- [2] Septentrional N.V., "Mosaic-H Technical Specifications," Septentrional GNSS Receiver Datasheet, 2022. [Online]. Available: <a href="https://www.septentrio.com">https://www.septentrio.com</a>
- [3] W. Zhang, M. J. Kim, and B. Lee, "Urban GNSS Accuracy Analysis for Autonomous Ground Vehicles," \*IEEE Transactions on Intelligent Transportation Systems\*, vol. 20, no. 6, pp. 2303–2312, June 2019. doi: 10.1109/TITS.2018.2868792
- [4] Y. Chen and J. Li, "GNSS Signal Quality under Forest Canopy: A Comparative Study of Single- and Dual-Frequency Receivers," \*Sensors\*, vol. 21, no. 8, p. 2703, Apr. 2021. Doi: 10.3390/s21082703.
- [5] RTCM Special Committee 104, "RTCM Recommended Standards for Differential GNSS Services Version 3.2," Radio Technical Commission for Maritime Services, Alexandria, VA, USA, 2013.
- [6] M. Portobello, "GNSS Solutions: Integration of GNSS and Inertial Navigation Systems," \*Inside GNSS\*, vol. 4, no. 3, pp. 26–28, 2009.
- [7] Dabove, P., & Di Pietra, V. (2023). Single- and Dual-Frequency GNSS Receivers for UAV-Based Mapping: Performance and Quality Assessment in an Urban Scenario. Sensors, 23(4), 2250. https://doi.org/10.3390/s23042250
- [8] Paziewski, J. (2022). Examining the Performance of New-Generation Low-Cost Dual-Frequency GNSS Receivers and Antennas for Positioning and Navigation. GPS Solutions, 26(4), 120. https://doi.org/10.1007/s10291-022-01310-7
- [9] F. Dovis, \*GNSS Interference Threats and Countermeasures\*, Artech House, 2015.

- [10] P. Misra and P. Enge, \*Global Positioning System: Signals, Measurements, and Performance\*, 2nd ed., Ganga-Jamuna Press, 2010.
- [11] C. Roumeliotis, A. Giannopoulos, and G. Bekiaris, "Reliable Telemetry in UAV Systems," in \*Proc. IEEE Aerospace Conf.\*, 2018, pp. 1–9. doi: 10.1109/AERO.2018.8396671.
- [12] S. Lo, D. De Lorenzo, and P. Enge, "GNSS Signal Challenges in Urban and Aerial Environments," in \*Proc. ION GNSS+\*, 2015
- [13] Holybro, "X500 V2 User Manual," 2022. [Online]. Available: https://holybro.com
- [14] ArduPilot Dev Team, "MAV Link Protocol Integration and Telemetry Streaming," \*ArduPilot Developer Docs\*, 2023. [Online]. Available: <a href="https://ardupilot.org/dev/docs/mavlink-introduction.html">https://ardupilot.org/dev/docs/mavlink-introduction.html</a>
- [15] L. Meier et al., "MAV Link: Micro Air Vehicle Communication Protocol," \*Autonomous Systems Lab\*, ETH Zurich, 2013. [Online]. Available: https://maylink.io
- [16] M. Shahriar, M. Marti, and T. Römer, "Low-Latency UAV Navigation Using MAV Link and Real-Time GNSS Corrections," in \*Proc. IEEE Aerospace Conf.\*, 2021, pp. 1–7. Doi: 10.1109/AERO50100.2021.9438343.
- [17] ArduPilot Dev Team, "MAV Link v2 Message Format," \*ArduPilot Documentation\*, 2023. [Online]. Available: https://ardupilot.org/dev/docs/maylink.html
- [18] D. Akos and J. Gao, "Real-Time Tuning of UAV PID Controllers over MAV Link Telemetry," in \*Proc. ION GNSS+\*, 2020, pp. 1934–1943.
- [19] F. Wang, D. Wu, X. Niu, and J. Liu, "Real-Time Kinematic Positioning of UAV Using Multi-Frequency GNSS and IMU Integration," \*IEEE Access\*, vol. 7, pp. 82894–82903, 2019. Doi: 10.1109/ACCESS.2019.2924358.

- [20] M. Khanafseh, B. Pervan, and Y. Chen, "Modeling the Effects of Multipath on GNSS Carrier Phase Tracking," \*IEEE Trans. Aerospace and Electronic Systems\*, vol. 46, no. 3, pp. 1058–1074, July 2010.
- [21] J. Zhang, K. Liu, and J. Wang, "GNSS Performance in Forest Environments: Effects of Multipath and Attenuation," \*Remote Sensing\*, vol. 10, no. 6, p. 869, 2018. Doi: 10.3390/rs10060869.
- [22] J. Zhang, K. Liu, and J. Wang, "GNSS Performance in Forest Environments: Effects of Multipath and Attenuation," \*Remote Sensing\*, vol. 10, no. 6, p. 869, 2018. Doi: 10.3390/rs10060869.
- [23]. M. Eren, Z. Kurtulgu, and A. Pirti, "Evaluation of the Repeatability and Accuracy of RTK GNSS under Tree Canopy," Jurnal Sylva Lestari, vol. 13, no. 2, pp. 392–405, 2025. Available: <a href="https://www.researchgate.net/publication/391566844">https://www.researchgate.net/publication/391566844</a>
  Evaluation of the Repeatability and Accuracy of RTK GNSS under Tree Canopy
- [24]. T. Suzuki et al., "Multi-Antenna GNSS Approach for UAVs in Urban Environments," Sensors, vol. 23, no. 4, p. 2092, 2023. Available: https://www.mdpi.com/1424-8220/23/4/2092
- [25] S. Kim et al., "Feedforward Fuzzy-PID Control for Air Flow Regulation of PEM Fuel Cell System," International Journal of Hydrogen Energy, vol. 40, no. 35, pp. 11686-11695, 2015.
- [26] Zhao, H., Li, Z., Wang, Q., Xie, K., Xie, S., Liu, M., & Chen, C. (2024). Improving performances of GNSS positioning correction using Multiview deep reinforcement learning with sparse representation. GPS Solutions, 28(3), 102. DOI: 10.1007/s10291-024-01626-6.
- [27] Li, B., Zhang, Z., & Miao, W. (2025). GNSS Real-Time Kinematic Positioning: Theory and Applications. Springer, Singapore. DOI: 10.1007/978-981-96-9116-6
- [28] Dabove, P., & Di Pietra, V. (2023). Single- and Dual-Frequency GNSS Receivers for UAV-Based

Mapping: Performance and Quality Assessment in an Urban Scenario. Sensors, 23(4), 2250. https://doi.org/10.3390/s23042250

[29] Paziewski, J. (2022). Examining the Performance of New-Generation Low-Cost Dual-Frequency GNSS Receivers and Antennas for Positioning and Navigation. GPS Solutions, 26(4), 120. https://doi.org/10.1007/s10291-022-01310-7

#### **Authors**



Mnar H. Saad is a postgraduate student in Global Navigation Satellite Systems (GNSS) at Beihang University, under the auspices of the Regional Centre for Space Science and Technology Education in Asia and the Pacific (RCSSTEAP).

She received her Bachelor of Science in Navigation Science and Space Technology from Beni Suef University, Egypt. Her current research focuses on developing high-fidelity lunar analog environments from remote sensing data to investigate how regolith dust, illumination extremes, and terrain conditions influence the reliability of rover navigation and mapping systems. She is particularly interested in integrating mission-derived regolith characterization data with simulation frameworks to support more resilient planetary exploration methods and enhance the scientific return of future lunar missions.



AHMED A. WASIU was born in Nigeria. He received the B.Eng. degree in electrical and computer engineering from the Federal University of Technology, Minna, Nigeria, in 2007, the M.Sc. degree in electrical and electronic engineering from the University of Ilorin, Nigeria, in 2014, and

the M.Sc. and Ph.D. degrees in global navigation satellite systems and satellite communications from Beihang University, Beijing, China, in 2016 and 2020, respectively.

From 2024, he has been an Ass. Professor with the Hangzhou International Innovation Institute, School of Electronic and Information Engineering (GNSS Department), Beihang University, Hangzhou, China. He has served as a visiting lecturer at several universities and has authored numerous articles in high-impact journals and international conferences. His research interests include GNSS signal processing, multipath mitigation, GNSS reflectometry, and AI-enhanced error correction techniques.



Odai Redhwan Othman is a postgraduate student in Space Technology Applications at Beihang University, under the auspices of the Regional Centre for Space Science and Technology Education in Asia and the Pacific (RCSSTEAP). He received his

Bachelor of Engineering in Telecommunication Engineering from the Civil Aviation University of China in 2024. His current research interests include Global Navigation Satellite Systems (GNSS), precise positioning algorithms for unmanned aerial vehicles (UAVs) in challenging low-altitude environments, and the development of robust path-planning strategies to ensure operational safety and efficiency.



Dr. YANG Dongkai born in 19th
July 1972 and is full professor in
School of Electronic and
Information Engineering,
Hangzhou International
Innovation Institute of Beihang
University. He graduated from
Beihang University and got Ph.D

degree in 2000, after that he joined the research team of GPS Center in Nanyang Technological University of Singapore and worked around 2 years. From 2003, he worked as an associate professor, and professor since 2010. His research interest is GNSS and its remote sensing applications, i.e. GNSS-R.

He published about 100 journal papers in English and 3 books on GNSS-R.

He currently is the Chinese Coordinator of China-Europe GNSS-R joint research group and the senior member of Chinese Electronics Institute